Materials Letters 280 (2020) 128580

Contents lists available at ScienceDirect

Materials Letters

journal homepage: www.elsevier.com/locate/mlblue

Effects of cooling conditions on the shape, microstructures, and material properties of SS308L thin walls built by wire arc additive manufacturing

Van Thao Le [a,b,*], Dinh Si Mai [b], Quang Huy Hoang [b]

[a] Institute of Research and Development, Duy Tan University, Da Nang 550000, Viet Nam
[b] Advanced Technology Center, Le Quy Don Technical University, Hanoi, Viet Nam

ARTICLE INFO

Article history:
Received 3 July 2020
Received in revised form 13 August 2020
Accepted 23 August 2020
Available online 27 August 2020

Keywords:
Additive manufacturing
Welding
Phase transformation
Microstructure
Mechanical properties

ABSTRACT

This research explores the effects of the free cooling and active cooling on the surface roughness, microstructures, and material properties of SS308L walls manufactured by wire arc additive manufacturing (WAAM). In the free cooling, a holding time of 30 seconds was used between two successive layers to cool down the wall by the natural air. On the other hand, in the active cooling, the compressed dry air was used for rapidly cooling the wall between two adjacent deposits. The results show that the walls built with the active cooling exhibits lower surface roughness and higher layer thickness when compared to those of the walls built with the free cooling. In both cases, the microstructure evolution of the walls is similar. A specified layer in the middle of the walls displays columnar dendrites of austenite growing vertically along the building direction and residual ferrite remaining in the boundaries of austenite. However, the spacing of secondary dendrite arms in the walls built with the active cooling is smaller, leading to a significant increase in microhardness and tensile strengths.

1. Introduction

Wire arc additive manufacturing (WAAM) is gaining increasing interests from different industrial sectors, because it features a high rate of material deposition and low costs of production and investment [1,2]. However, the arc used in WAAM generates high heat input, and WAAM components undergo complex thermal cycles and high heat accumulation [3]. Thereby, the shape, microstructures, and mechanical properties of WAAM parts are difficult to be controlled.

To deal with the heat accumulation issue in WAAM, Yin et al. [4] used a mixture of CaF_2 and acetone as the activating flux, which was manually coated on the top surface of layers, in WAAM of Ti-6Al-4V walls. Silva et al. [5] designed a water-cooling system, in which the built part was dipped in the tank of water during the WAAM process. However, this cooling system restricted the flexibility of WAAM systems. Hackenhaar et al. [6] employed compressed dry air for the cooling and assessed its impact on the heat accumulation in WAAM of ER70S-6 steel walls. They observed that this cooling approach allowed restricting the gradual augmentation of the interpass temperature.

From the above studies, it is found that the active cooling using the compressed dry air (CDAir) seems more effective and easier to be implemented than other ones. Moreover, the use of CDAir for the cooling has less impact to the environmental than CO_2 and argon gases. In this paper, the CDAir is also employed to cool down the workpiece during the WAAM process of SS308L parts that is rarely reported in the literature [7]. The influence of such a cooling method on the shape, microstructures, and material properties of WAAM SS308L walls was analyzed.

2. Materials and methods

In this study, two thin walls were built on low-carbon steel substrates by a WAAM system (a robotic welding system TA 1400 of Panasonic). A commercial 1-mm-diameter SS308L wire was used as the raw material. The wire's chemical composition comprises (19.5–21)%Cr, (9.0–11.0)%Ni, (0.30–0.65)%Si, (1.0–2.5)%Mn, (≤0.50)%Mo, (≤0.75)%Cu, (≤0.03)%C, (≤0.03)%P, (≤0.03)%S, and (balance)%Fe. SS308L is a type of austenite stainless steels [8–10], which is extensively employed in different industrial sectors, for example, gas, oil, mining, and steamship building industries.

The walls were built by depositing twenty layers successively in the same direction (Fig. 1a) and using the same processing parameters, including a voltage of 20 V, a welding current of 122 A, and a traveling speed of 0.368 m/min [11]. The molten pool was pro-

* Corresponding author at: Advanced Technology Center, Le Quy Don Technical University, Hanoi, Vietnam.
E-mail address: thaomta@gmail.com (V.T. Le).

https://doi.org/10.1016/j.matlet.2020.128580
0167-577X/

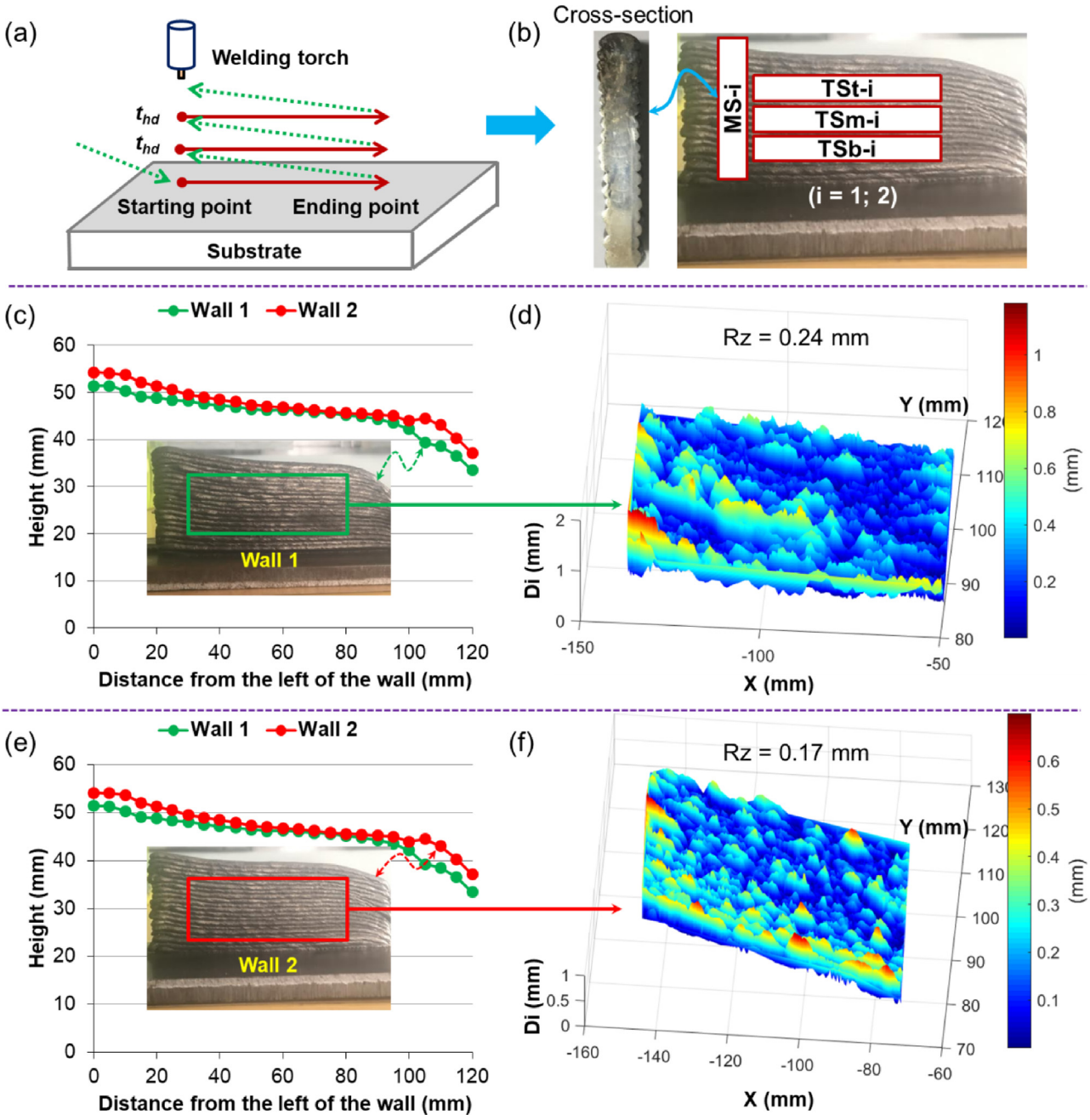

Fig. 1. (a) The deposition strategy, (b) positions for cutting the microstructure specimen (MS-i) and three horizontal tensile specimens (TSt-i, TSm-i, and TSb-i), the shape and surface roughness of the wall (1) (c and d) and the wall (2) (e and f).

tected by a shielding gas of 99.9% argon. The wall (1) (Fig. 1c) was built with the free cooling, in which a holding time t_{hd} = 30 seconds was used between successive layers to cool down the wall by the natural air. On the other hand, the wall (2) (Fig. 1e) was built with the active cooling using the CDAir for rapidly cooling the wall between two adjacent layers.

The walls' shape was acquired by using a non-contact 3D digitizer to estimate the surface roughness of the walls based on the method reported in [12]. To compare the effect of two cooling methods, the material properties in the middle region of the walls were particularly analyzed. For each wall, a specimen (MS-i) used to observe the microstructure and microhardness, and three horizontal tensile specimens (TSt-i, TSm-i, and TSb-i) were extracted (Fig. 1b), herein i = 1 and 2 for the walls (1) and (2), respectively. The microstructures were analyzed by an optic microscope. The microhardness was measured by a Vickers microhardness tester. The tensile strengths were measured by a tensile testing machine. All tensile tests were implemented at room temperature and with a displacement speed of the crosshead of 10 mm/min.

3. Results and discussion

The shape and surface roughness of the walls are shown in Fig. 1. It is firstly found the shape of two walls is similar. However, the wall (2) reveals relatively higher height (the red curve vs. the green curve). The surface roughness of the wall (2) (Rz = 0.17 mm) is lower than that of the wall (1) (Rz = 0.24 mm). In fact, the wall (1) was built with the free cooling, in which the temperature of the current deposited layer was gradually cooled

down by the natural air to a value superior to 120°C [6], whereas, the current deposited layer of the wall (2) was rapidly cooled down to the ambiance temperature by the CDAir. Thus, the heat accumulation and solidification time in the wall (1) must be higher than those in the wall (2), leading to a strong overflow of the molten pool, thinner layer thickness, and higher surface roughness in the wall (1) [12].

In terms of microstructures, two walls reveal similar evolution of microstructures (Fig. 2). The microstructures of WAAM SS308L walls are dominantly composed of columnar dendrites of austenite (in white) and residual ferrite (in black), which exists in the boundaries of austenite. The solidification in WAAM SS308L walls occurs according to the FA mode [7]: Firstly, primary ferrite phases formed. Then they were progressively replaced by austenite phases during the solidification period. In a specific layer, finer columnar structures in the bottom zone gradually develop along the building direction and transform into coarser structures in the top of the layer. The secondary dendrites of austenite appear visibly farther away the bottom of the layer.

In both walls, the average spacing of secondary dendrite arms (SSDA) increases from the bottom to the top of a layer (Fig. 2). However, the average SSDA in the second wall is smaller than that in the first wall. Indeed, SSDA decreases with an augmentation in the cooling rate [13,14]. As aforementioned, the cooling rate in the first wall is obviously lower, because the heat accumulation in the first wall is higher. Therefore, SSDA in the first wall is larger. Moreover, in the middle of the second wall, SSDA is relatively similar in all layers, while SSDA slightly increases in higher layers in

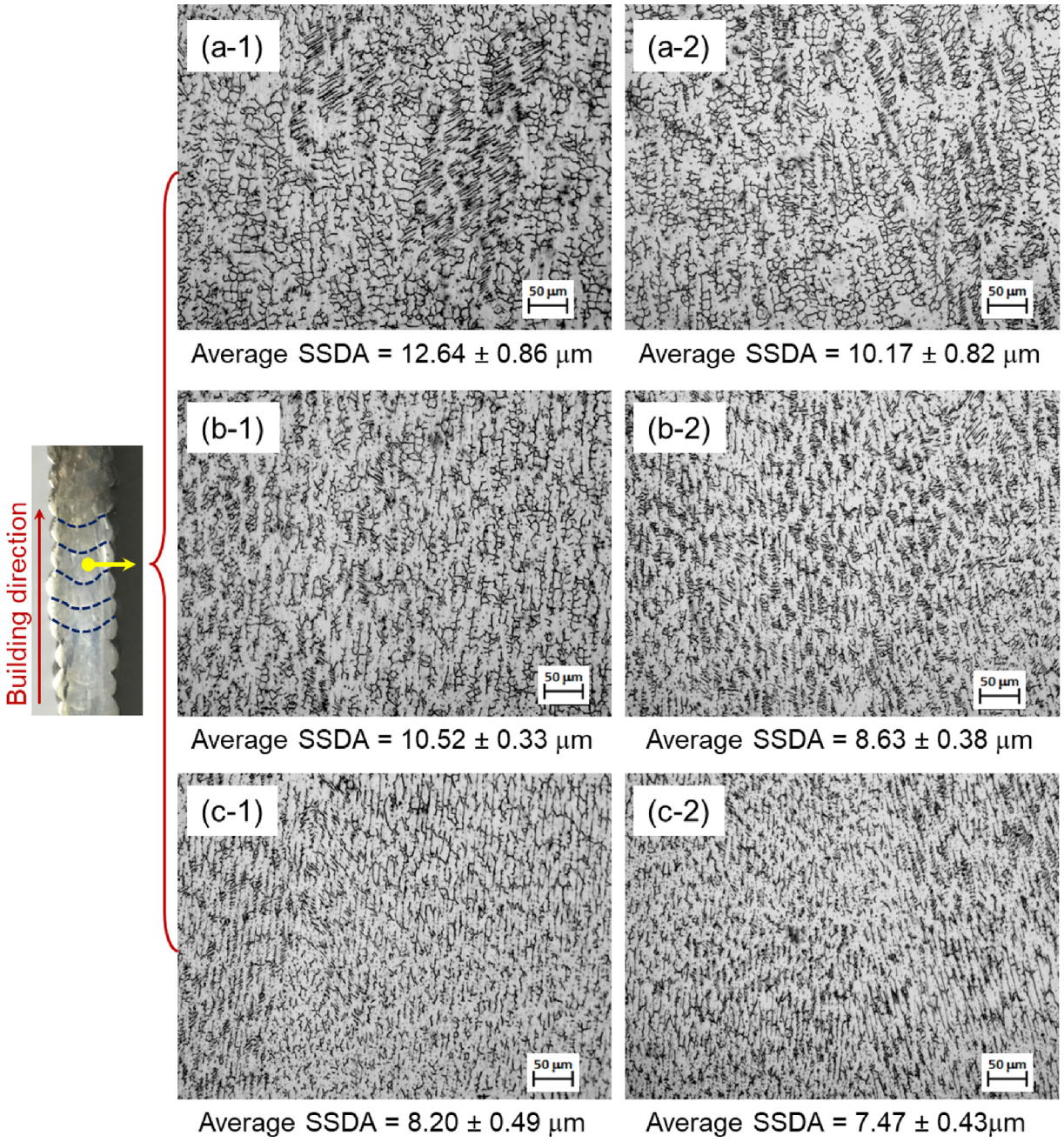

Fig. 2. Microstructure of a specified layer in the middle region of WAAM SS308L walls: (a-i) in the top, (b-i) in the middle, and (c-i) in the bottom of the layer, i = 1 and 2 for the wall (1) and (2).

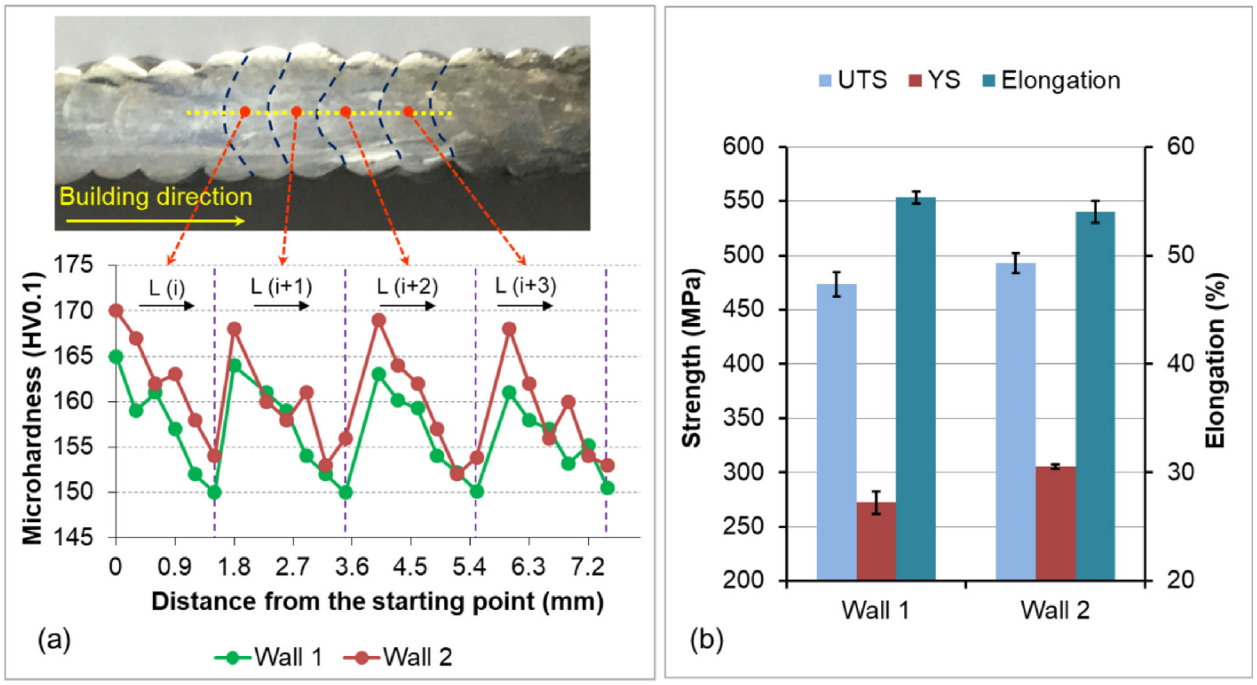

Fig. 3. (a) Microhardness measured in the middle region and (b) tensile properties of the walls.

the middle of the first wall. In the first wall, the heat accumulation increases and the heat dissipation decreases when the layer number increases, thereby the cooling rate in the higher layers is lower than that in the lower layers. On the other hand, in the second wall, there is no substantial difference of the interlayer temperature during the build, because the second wall was rapidly cooled down by the CDAir between two adjacent deposits.

The microhardness was measured in the center of four successive layers in the middle region of the walls (Fig. 3a). The microhardness of the wall (2) is relatively higher than that of the wall (1). The average microhardness of the wall (2) in the middle region is 160.04 ± 5.58 (HV0.1), whereas that value of the wall (1) is 156. 56 ± 4.72 (HV0.1). In addition, in a layer, the hardness decreases from the bottom to the top of the layer.

The tensile strengths (YS and UTS) of the wall (2) are also higher than those of the wall (1) (Fig. 3b). The average value of YS and UTS of the wall (2) are 305.67 ± 2.08 (MPa) and 492.67 ± 9.02 (MPa), respectively, whereas YS = 272.33 ± 10.07 (MPa) and UTS = 472.3 3 ± 11.06 (MPa) for the wall (1). On the other hand, the elongation of the wall (1) is relatively higher than that of the wall (2) (55.33 ± 0.58% vs. 54 ± 1%).

The results on the hardness and tensile strengths are logical agreement with the microstructure evolution in the walls, because the SSDA in the middle region of the wall (1) is larger than that of the wall (2). Within a layer, the SSDA also increases from the bottom to the top of the layer. According to the Hall-Petch relation, the tensile strengths and hardness in the middle region of the wall (1) are logically lower than those of the wall (2).

4. Conclusions

In this paper, the effects of the active cooling method on the shape, microstructures, hardness, and tensile properties of WAAM SS308L walls were assessed. The walls built with the active cooling reveal higher layer thickness and lower surface roughness than those of the walls built with the free cooling method. Moreover, the average SSDA in the middle region of the walls built with the active cooling method is smaller, leading to higher hardness and higher tensile strengths. The average YS and UTS of the walls built with the active cooling are 305.67 ± 2.08 (MPa) and 492.67 ± 9.02 (MPa), respectively, compared to YS = 272.33 ± 10.07 (MPa) and UTS = 472.33 ± 11.06 (MPa) of the walls built with the free cooling. Therefore, the active cooling method using the CDAir can be considered as a good solution to improve the external and internal qualities of WAAM SS308L walls and the productivity.

CRediT authorship contribution statement

Van Thao Le: Conceptualization, Methodology, Investigation, Validation. **Dinh Si Mai:** Investigation, Validation. **Quang Huy Hoang:** Investigation, Validation.

Declaration of Competing Interest

The authors declare that they have no known competing financial interests or personal relationships that could have appeared to influence the work reported in this paper.

Acknowledgement

This research is funded by Vietnam National Foundation for Science and Technology Development (NAFOSTED) under grant number 107.99-2019.18.

References

[1] F. Martina, J. Ding, S. Williams, A. Caballero, G. Pardal, L. Quintino, Addit. Manuf. 25 (2019) 545–550.
[2] B. Wu, Z. Pan, D. Ding, D. Cuiuri, H. Li, J. Xu, J. Norrish, J. Manuf. Process. 35 (2018) 127–139.
[3] C.R. Cunningham, J.M. Flynn, A. Shokrani, V. Dhokia, S.T. Newman, Addit. Manuf. 22 (2018) 672–686.
[4] B. Yin, H. Ma, J. Wang, K. Fang, H. Zhao, Y. Liu, Mater. Lett. 190 (2017) 64–66.
[5] L.J. da Silva, D.M. Souza, D.B. de Araújo, R.P. Reis, A. Scotti, Int. J. Adv. Manuf. Technol. 107 (2020) 2513–2523.
[6] W. Hackenhaar, J.A.E. Mazzaferro, F. Montevecchi, G. Campatelli, J. Manuf. Process. 52 (2020) 58–65.

[7] V.T. Le, D.S. Mai, Mater. Lett. 271 (2020) 127791.
[8] B. Al-Mangour, Nova Science Publishers (2015).
[9] B. AlMangour, D. Grzesiak, T. Borkar, J.M. Yang, Mater. Des. 138 (2018) 119–128.
[10] B. AlMangour, D. Grzesiak, J.-M. Yang, J. Alloys Compd. 728 (2017) 424–435.
[11] V.T. Le, D.S. Mai, T.K. Doan, Q.H. Hoang, Transp. Commun. Sci. J. 71 (2020) 431–443.
[12] J. Xiong, Y. Li, R. Li, Z. Yin, J. Mater. Process. Technol. 252 (2018) 128–136.
[13] H. Yin, S.D. Felicelli, Acta Mater. 58 (2010) 1455–1465.
[14] L. Wang, J. Xue, Q. Wang, Mater. Sci. Eng. A 751 (2019) 183–190.